SUPPLEMENTAL DATA

PET/CT scanner specifications

Subjects and phantoms were scanned on a Siemens Biograph mCT 128 PET scanner at the Melbourne Brain Centre Imaging Unit, the University of Melbourne. All data were recorded in three dimensions and saved in list-mode before reconstruction.

Subject scanning

Cross-sectional study

A total of 89 subjects were selected from the Australian Imaging, Biomarker and Lifestyle study (AIBL) study. The subjects were chosen to ensure that the datasets were evenly distributed between Aβ- and Aβ+ groups with matching age and gender. All subjects were scanned for Aβ by injecting [^{18}F]-florbetapir radiotracer dose of 370±10%MBq 50 minutes prior to 20 minutes of continuous scanning (**Supplemental Table 1**).

Longitudinal study

From the AIBL FLUTE longitudinal study, 79 subjects each with three longitudinal data points were selected. Subjects were injected with [^{18}F]-flutemetamol radiotracer dose of 185±10%MBq 90 minutes prior to 20 minutes of continuous scanning. The first and second follow-up scans were acquired 1.61 ± 0.14 and 3.21 ± 0.21 years after the baseline scan, respectively.

Ethics approval and consent to participate in this study were approved by the Austin Health Human Research Ethics Committee (HREC/18/Austin/201)

Both cross-sectional and longitudinal reconstructions were computed using the Siemens' e7 toolbox with attenuation, decay, scatter and random corrections. Cross-sectional datasets were reconstructed at a voxel size of 4.07 mm × 4.07 mm × 2.01 mm and dimensions of 200 × 200 × 109 voxels. Longitudinal datasets were reconstructed at a voxel size of 1.99 mm × 1.99 mm × 3.00 mm and dimensions of 256 × 256 × 148 voxels.

Phantom scanning

A cylindrical phantom was used to measure the axial and radial PET spatial resolution of a given reconstruction configuration by calculating the full width at half maximum (FWHM) along each direction. The phantom was filled with 64.7 MBq of ^{18}F, and placed at the centre of the scanner FOV, with the long axis parallel to the axis of the scanner. One end of the phantom was lifted to create a small angle with the scanner axis, in order that the phantom edge intersects the image matrix obliquely in different slices. The tilted phantom was scanned for 60 minutes. Each phantom scan was reconstructed with a set of reconstruction configurations and uploaded to the Society of Nuclear Medicine and Molecular Imaging's (SNMMI) phantom analysis toolkit (http://www.snmmi.org/PAT) to calculate axial and radial resolutions of each configuration in FWHMs. The average of the axial and radial resolution was the FWHM associated with the given reconstruction configuration.

Supplemental Table 1: Demographics of Cross-sectional and Longitudinal study datasets.

Study Type	Cross-sectional		Longitudinal	
Aβ group	Aβ-	Aβ+	Aβ-	Aβ+
Sample size	44	45	46	33
Sex. F (%)	26 (59)	26 (58)	22 (47.83)	13 (39.39)
Age ± SD	71 ± 3.77	70.78 ± 3.96	71.91 ± 4.51	74.00 ± 5.59
% Right hand	91	91	89*	84*
% APOE4	21*	70 **	15	39
CU, MCI, AD	41, 0, 0***	37, 4, 0****	41, 4, 1	24, 4, 4*
MMSE ± SD	27.9 ± 1.22	27.71 ± 1.33	29.09 ± 0.98	27.52 ± 2.83
CDR ± SD	0 ± 0*	0.03 ± 0.13	0 .05 ± 0.19	0.17 ± 0.30
CDR-SoB ± SD	0.01 ± 0.08*	0.09 ± 0.22	0.18 ± 1.03	0.79 ± 1.90

Demographics marked with * are missing values from some subjects, where the number of * corresponds to the number of subjects missing. F = Female, SD = Standard Deviation, APOE4 = Apolipoprotein E4, CU = Cognitively unimpaired, MCI = Mild Cognitively Unimpaired, AD = Alzheimer's Disease, MMSE = Mini-Mental State Examination, CDR = Clinical Dementia Rating, CDR-SoB = Clinical Dementia Rating Scale Sum of Boxes.

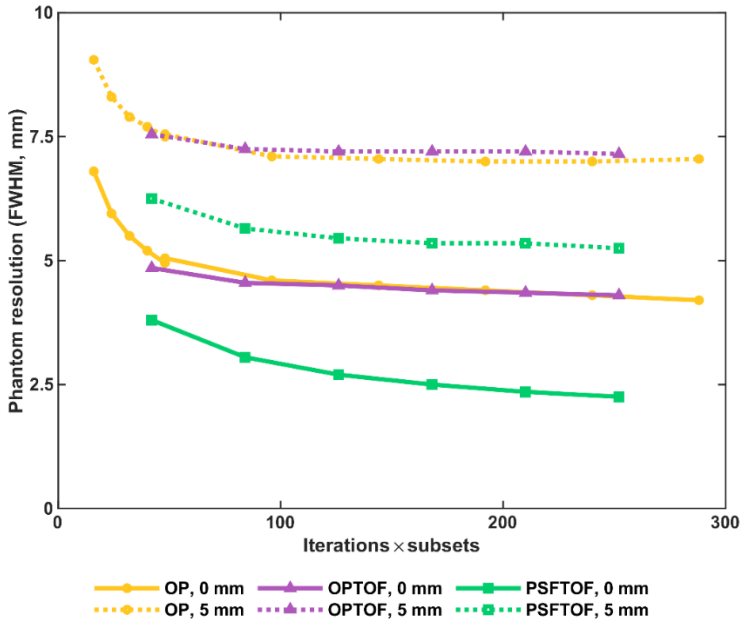

Supplemental Figure 1: Algorithm convergence vs phantom resolution. Change in spatial resolution, FWHM, of a barrel phantom as a function of algorithm convergence, indicated by the product of subsets, s, and iterations, i. Each marker indicates reconstruction of a barrel phantom using a different reconstruction protocol, defined by the algorithm, subsets, iterations and post-reconstruction Gaussian smoothing.

Smoothing effect on Aβ quantitation.

Supplementary Supplemental Figure 2 shows changes in mean Aβ CL for each reconstruction group after the images are smoothed with a 5 mm post-reconstruction Gaussian filter. As per Supplementary Supplemental Figure 2**,** post-reconstruction smoothing impacted the CL of the Aβ+ group, with the application of a 5 mm smoothing filter reducing the Aβ+ group's mean CL value for every reconstruction configuration (Supplementary Supplemental Figure 2, red markers). However, for the Aβ- group, the change in mean CL after the application of a 5 mm smoothing filter was negligible for all reconstruction configurations (Supplementary Supplemental Figure 2, blue markers).

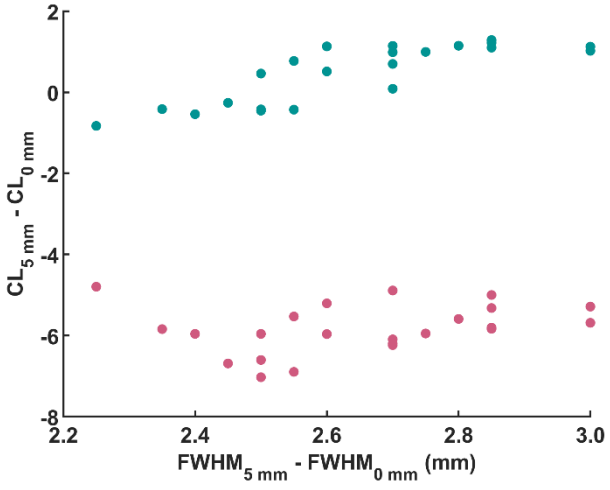

Supplemental Figure 2: The impact of post-reconstruction smoothing on Aβ CL. Change in mean CL for each reconstruction group after the application of a 5 mm post-reconstruction Gaussian smoothing. Aβ- and Aβ+ groups are shown separately. Note: Error bars are not included as they are too small to be legible.

Cohen's d analysis

To analyse the impact of the reconstruction configuration on the separation between the CLs of the Aβ- and Aβ+ groups, the effect size of the difference in mean CL value between the groups as measured by Cohen's d was compared against the FWHM value of the reconstruction method (Supplemental Figure 3). The maximum effect size between the groups was achieved by PSFTOF (10*i*, 21*s*) with 1 mm smoothing, with similar effect sizes for all PSFTOF reconstructions with 0 mm and 1 mm smoothing. Effect sizes decreased with FWHM value, irrespective of the reconstruction method and the level of smoothing used.

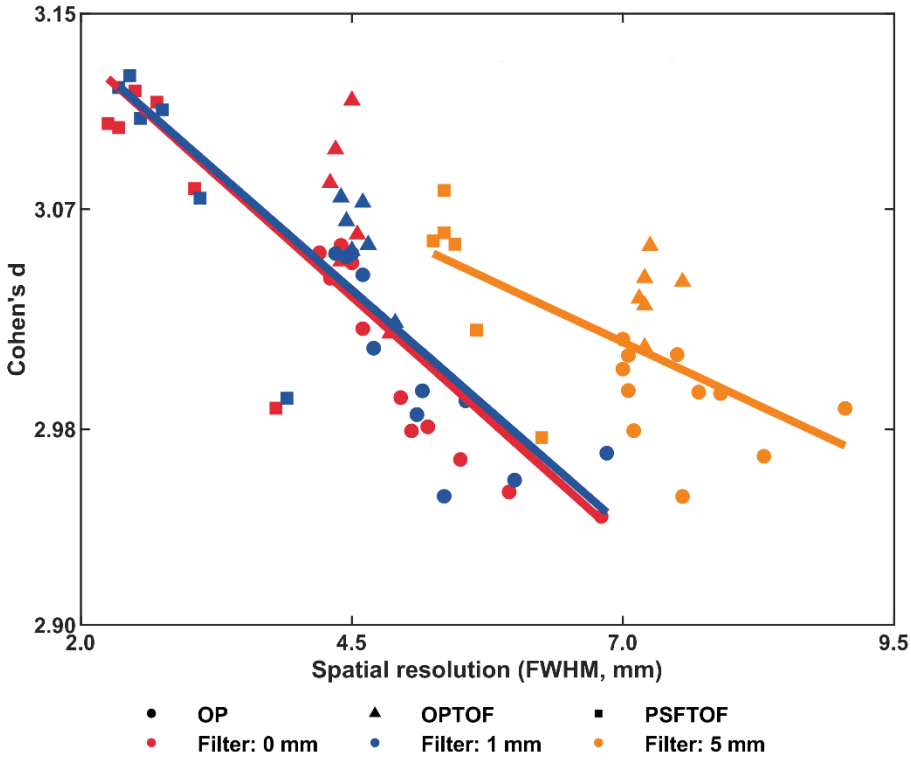

Supplemental Figure 3: Spatial resolution versus the effect size of the difference in mean CL between Aβ- and Aβ+ groups as measured by Cohen's d. The impact of the spatial resolution of each reconstruction configuration on the effect size of the difference in mean CL between Aβ+ and Aβ- groups. Correlations between FWHM and Cohen's d for different post-reconstruction Gaussian smoothing amounts are -0.818, -0.862, and -0.622, for 0 mm, 1 mm and 5 mm filters, respectively. Lines of best fit are depicted by red (0 mm), blue (1 mm) and orange (5 mm).

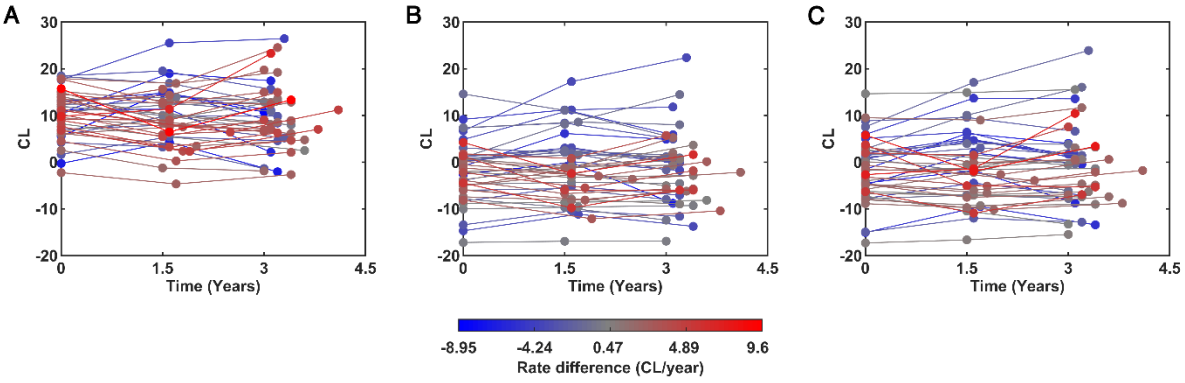

Supplemental Figure 4: Summary of longitudinal Aβ- CL values reconstructed with low-, medium- and high-resolution reconstruction protocols. Each line denotes a single subject's CL over time, with colour determined by the difference in accumulation rate between the first and second scanning intervals.

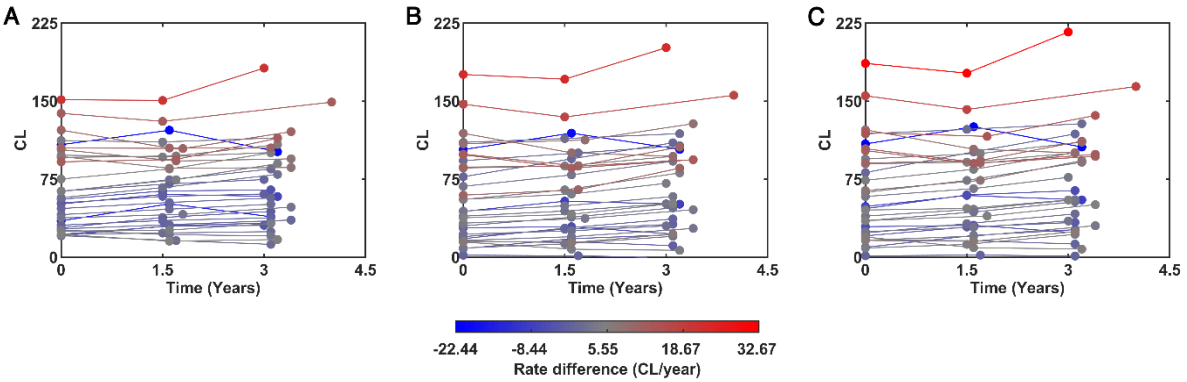

Supplemental Figure 5: Summary of Aβ+ longitudinal data reconstructed with low-, medium- and high-resolution reconstruction protocols. Each subject has 3 CL values over time. Impact of spatial resolution on Aβ accumulation rate difference is depicted by the colour coding of each subject's line, determined by the change in accumulation rate between the first and second scanning intervals.

Supplemental Table 2: Comparison of spatial resolution sensitivity to longitudinal changes: Estimated number of Aβ accumulators in the Aβ- and Aβ+ cohorts. Accumulation rates significantly greater than 0 CL/year, and significantly greater than 2 CL/year.

Reconstruction type (Algorithm, resolution)	Number of identified Aβ accumulators (Threshold=0 CL/year, Aβ-)	Number of identified Aβ accumulators (Threshold=2 CL/year, Aβ-)	Number of identified Aβ accumulators (Threshold=0, CL/year, Aβ+)	Number of identified Aβ accumulators (Threshold=2 CL/year, Aβ+)
Low resolution (OP, 7.05 mm)	17	6	26	22
Medium resolution (OPTOF, 4.55 mm)	27	6	26	25
High resolution (PSFTOF, 3.05 mm)	27	6	25	24

Supplemental Table 3: Reconstruction configurations used in the cross-sectional analysis and their relevant Aβ-PET CL and FWHM values.

Reconstruction method	Iterations	Subsets	Filter size (mm)	FWHM (mm)	Mean CL of Aβ- group	SD of Aβ- group	Mean CL of Aβ+ group	SD of Aβ+ group
PSFTOF	12	21	0	2.25	-24.35	13.50	63.72	37.58
PSFTOF	10	21	0	2.35	-24.56	13.75	63.81	37.66
PSFTOF	12	21	1	2.35	-24.26	13.45	63.88	37.43
PSFTOF	10	21	1	2.45	-24.66	13.52	63.92	37.56
PSFTOF	8	21	0	2.5	-24.49	13.51	63.78	37.49
PSFTOF	8	21	1	2.55	-24.34	13.47	63.85	37.62
PSFTOF	6	21	0	2.7	-24.53	13.50	63.67	37.53
PSFTOF	6	21	1	2.75	-24.60	13.46	63.66	37.62
PSFTOF	4	21	0	3.05	-23.82	13.21	62.94	37.42
PSFTOF	4	21	1	3.1	-23.74	13.16	63.16	37.56
PSFTOF	2	21	0	3.8	-23.97	12.67	59.63	37.28
PSFTOF	2	21	1	3.9	-24.05	12.77	59.45	37.14
OP	2	24	0	4.2	-23.92	12.66	60.40	36.78
OPTOF	12	21	0	4.3	-24.21	12.75	57.74	35.22
OP	10	24	0	4.3	-24.00	12.61	60.32	36.93
OPTOF	10	21	0	4.35	-24.29	12.75	57.89	35.15
OP	12	24	1	4.35	-23.86	12.52	60.42	36.80
OPTOF	12	21	1	4.4	-24.20	12.62	57.46	35.20
OP	8	24	0	4.4	-24.01	12.69	60.22	36.68
OPTOF	8	21	0	4.4	-23.57	12.79	57.74	35.31
OPTOF	10	21	1	4.45	-24.29	12.69	57.35	35.29
OP	10	24	1	4.45	-24.06	12.65	60.27	36.81
OP	8	24	1	4.5	-24.04	12.66	60.16	36.72
OPTOF	6	21	0	4.5	-24.13	12.66	58.02	34.92
OP	6	24	0	4.5	-23.69	12.43	60.41	36.80
OPTOF	8	21	1	4.5	-23.64	12.88	57.19	34.98
OPTOF	4	21	0	4.55	-24.09	12.46	57.08	35.21
OPTOF	6	21	1	4.6	-24.17	12.49	57.26	35.16
OP	6	24	1	4.6	-23.70	12.41	60.05	36.70
OP	4	24	0	4.6	-23.36	12.48	60.03	36.80
OPTOF	4	21	1	4.65	-24.10	12.39	57.07	35.29
OP	4	24	1	4.7	-23.38	12.49	59.88	36.84
OPTOF	2	21	0	4.85	-23.72	12.29	55.85	35.01
OPTOF	2	21	1	4.9	-23.78	12.23	55.49	34.83
OP	2	24	0	4.95	-21.46	11.97	59.75	36.27

OP	12	4	0	5.05	-21.31	12.11	60.41	36.66
OP	2	2	1	5.1	-21.46	11.95	59.97	36.48
OP	12	4	1	5.15	-21.22	12.22	60.28	36.30
OP	10	4	0	5.2	-20.58	12.03	60.25	36.23
PSFTOF	12	21	5	5.25	-23.22	12.71	58.43	35.40
PSFTOF	10	21	5	5.35	-23.54	12.65	58.12	35.15
PSFTOF	8	21	5	5.35	-23.39	12.55	57.94	35.25
OP	10	4	1	5.35	-20.60	11.88	59.79	36.44
PSFTOF	6	21	5	5.45	-23.53	12.45	57.72	35.31
OP	8	4	0	5.5	-19.35	12.33	59.88	35.51
OP	8	4	1	5.55	-19.49	12.21	59.91	35.31
PSFTOF	4	21	5	5.65	-23.30	12.11	56.97	35.40
OP	6	4	0	5.95	-17.06	12.22	59.34	34.30
OP	6	4	1	6	-17.16	12.20	59.30	34.27
PSFTOF	2	21	5	6.25	-24.23	11.52	52.94	34.63
OP	4	4	0	6.8	-12.96	12.71	57.89	31.41
OP	4	4	1	6.85	-13.15	12.54	57.88	31.26
OP	8	24	5	7	-22.87	11.27	55.02	34.71
OP	10	24	5	7	-22.85	11.24	55.43	34.76
OP	12	24	5	7.05	-22.63	11.23	55.41	34.72
OP	6	24	5	7.05	-22.91	10.92	54.88	34.88
OP	4	24	5	7.1	-22.90	11.03	54.07	34.65
OPTOF	12	21	5	7.15	-22.94	11.28	52.42	33.10
OPTOF	6	21	5	7.2	-23.14	11.30	51.93	32.99
OPTOF	10	21	5	7.2	-23.06	11.39	52.09	32.87
OPTOF	8	21	5	7.2	-22.42	11.64	52.15	32.84
OPTOF	4	21	5	7.25	-23.39	11.10	50.88	32.37
OP	2	24	5	7.5	-21.89	10.47	52.85	33.34
OPTOF	2	21	5	7.55	-23.64	10.81	49.62	32.15
OP	12	4	5	7.55	-21.76	10.58	53.39	33.93
OP	10	4	5	7.7	-21.01	10.66	53.64	33.42
OP	8	4	5	7.9	-19.89	10.90	53.92	32.94
OP	6	4	5	8.3	-17.48	11.21	53.50	31.74
OP	4	4	5	9.05	-13.79	11.56	53.09	29.32